

Inverse four-domain twisted nematic liquid crystal display fabricated by the enhancement of azimuthal anchoring energy

Soo In Jo,¹ Sang-Woong Choi,¹ You-Jin Lee,² Yeon-Kyu Moon,² Young-Cheol Yang,³ Chang-Jae Yu,^{1,2} and Jae-Hoon Kim^{1,2,a)}

¹Department of Electronic Engineering, Hanyang University, Seoul 133-791, Korea

²Department of Information Display Engineering, Hanyang University, Seoul 133-791, Korea

³Liquid Crystal Institute, Kent State University, Kent, Ohio 44242, USA

(Received 4 November 2010; accepted 21 January 2011; published online 19 April 2011)

An inverse four-domain twisted nematic (IFDTN) liquid crystal (LC) display was fabricated by enhancing the azimuthal anchoring energy of the alignment layers. By stacking a vertical alignment layer onto a planar alignment layer, we increased the azimuthal anchoring energy by approximately 17-fold times compared to that with vertical alignment only. Due to the enhanced azimuthal anchoring energy, we were able to achieve a four-domain twisted nematic LC structure without dopant via the application of an external voltage. A simulation of the LC molecular orientation with respect to the azimuthal anchoring energy, the viewing angle characteristics, and the switching behavior of the IFDTN LC are presented. © 2011 American Institute of Physics. [doi:10.1063/1.3559262]

I. INTRODUCTION

It is well known that high optical performance, including high transmittance, high contrast ratio, fast response time, and wide viewing angle, are required in liquid crystal displays (LCDs), especially for large area displays such as high definition televisions. Twisted nematic (TN) mode is most commonly used in LCDs due to its simple fabrication process, fast response time, and high transmittance.¹ However, it is difficult to obtain a completely dark state when applying a field under crossed polarizers due to the hard anchoring of the alignment layers. For a completely dark state, an inverse TN (ITN) structure was developed using a vertical alignment layer and a nematic LC with a chiral dopant.² However, it is difficult to obtain symmetric viewing angle characteristics in TN and ITN because the optic axes in the midplanes of the cells are uniformly tilted in a single direction.

To overcome this limitation of TN and ITN, many techniques have been proposed for the production of LC multi-alignment, such as in-plane switching (IPS),³ fringe field switching (FFS),⁴ vertical alignment (VA) with a patterned electrode,^{5,6} and four-domain TN (FDTN).⁷ The IPS and FFS modes provide wide viewing angle characteristics, but their dynamic responses are relatively slow, and the contrast ratios are less than those of the TN, FDTN and VA modes.⁸ The multi-domain VA mode with compensation films also demonstrates good viewing characteristics, fast response time, and high contrast ratio, but the transmittance is lower than those of the TN and FDTN modes. In particular, the VA mode provides an excellent contrast ratio due to the vertical alignment of LCs in the absence of an external voltage field.

Schadt *et al.* proposed the photo-alignment method for LCDs with linearly polymerized photopolymers,⁹ and, as continuing researches, FDTN LCDs were demonstrated by patterning the alignment surface using linear photo-polymerization

technology for wide viewing angle.^{10,11} This method has simple process for mass-products and wide viewing angle characteristics, but the contrast ratio is lower than VA modes.

Therefore, we can anticipate achieving the best electro-optical performance by combining the vertical alignment in the initial state and the FDTN structure with an external field, specifically, inverse FDTN (IFDTN). Figure 1 shows the schematic diagrams of the IFDTN mode using LCs with negative dielectric anisotropy and a reverse rubbing process,¹² before and after application of an electric field. Without an external field, the LCs are aligned in the vertical direction with a pretilt angle due to the rubbed vertical

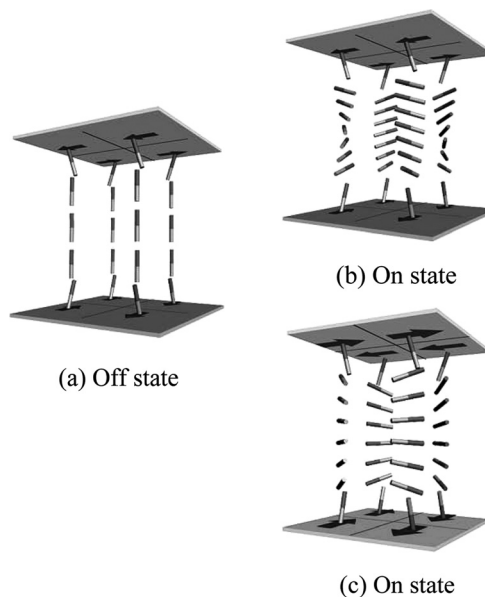


FIG. 1. Schematic diagrams of the IFDTN mode using LCs with a negative dielectric anisotropy (a) before and after the application of an electric field with (b) stacked alignment layer and (c) vertical alignment layer alone.

^{a)}Electronic mail: jhoon@hanyang.ac.kr.

alignment layer [Fig. 1(a)]; the LC began to tilt and twist due to the different rubbing directions on the bottom and top substrates over a specific critical field [Fig. 1(b)]. An IFDTN has been attempted by employing photo-alignment¹³ and a micro-rubbing process¹⁴ on the vertical alignment layer. However, even though the vertical alignment of LCs with four different pretilt angles has been achieved, after application of the electric field, the pixels displayed a uniform alignment instead of a twisted alignment, as shown in Fig. 1(c). Patel and Cohen reported that this was a result of the weak azimuthal anchoring energy of the vertical alignment layer. In order to solve this problem, a chiral dopant has been added to nematic LCs. However, this addition requires a cumbersome four rubbing processes in each substrate for four different domains.¹⁵

In this article, we fabricated the IFDTN LCD for the first time within our first hand knowledge by stacking the vertical alignment layer onto the planar alignment layer in order to improve the azimuthal anchoring energy. Due to the enhanced anchoring energy, we are able to achieve twisted nematic structures without a dopant and additional two rubbing process in each substrate. The simulation of the LC molecular orientation depending on the azimuthal anchoring energy, the viewing angle characteristics, and the switching behavior of the IFDTN LC are presented.

II. EXPERIMENTAL

Figure 2 shows the schematic diagram of the sample fabrication process. Initially, indium tin oxide (ITO) glass substrates were cleaned using detergent and rinsed with deionized water. Next, a planar alignment material (SE7492, Nissan Chem.) was spin coated as a first layer [Fig. 2(a)] and baked onto a hot plate at 210°C for imidization. The second vertical alignment material (AL1H659, JSR) was diluted with mixtures of n-methyl-pyrrolidone, butyrolactone, and butoxyethanol in order to control the layer thickness; the diluted material was spin coated onto the first alignment layer and baked on a hot plate at 180°C, as shown in Fig. 2(b). The substrate was then rubbed in an anti-parallel direction by shifting the shadow mask, as shown in Fig. 2(c). The two substrates were then assembled as a conventional TN cell. Samples were prepared using different concentra-

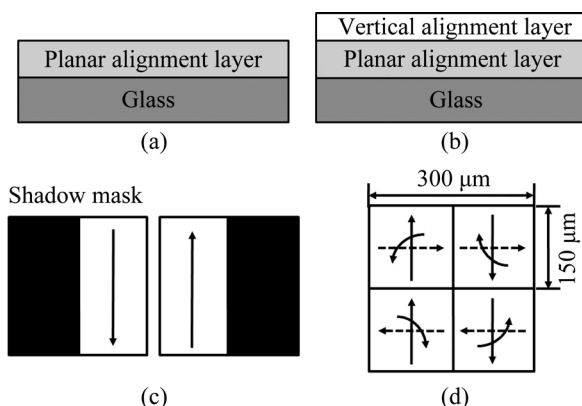


FIG. 2. Schematic diagrams of the (a), (b) stacked alignment layer system, (c) reverse rubbing process, and (d) top view of the sample.

tions of the vertical alignment material in order to control the azimuthal anchoring energy. Kim *et al.* reported that the pretilt angle of the LC on the stacked alignment layers increases with an increase in the thickness of the second layer, leading to saturation.¹⁶ We found that the pretilt angle was saturated at approximately 87° if the concentration of the vertical alignment material was greater than 5 wt %. Figure 2(d) shows the top view of our IFDTN sample; the dashed and solid arrows indicate the rubbing directions on the top and bottom substrates, respectively. And the curved lines represent twisting sense in each sub-domains since we used LCs without dopant, we can get two different twisting senses with two kinds of azimuthal directions. The pixel size was approximately 300 μm × 300 μm, and the size of the sub-pixel was approximately 150 μm × 150 μm. A cell gap of 4 μm was maintained by glass spacers, and an LC with negative dielectric anisotropy (MLC-6608, Merck) was injected via capillary force at the isotropic phase temperature. For comparison, we fabricated a cell with only a vertical alignment layer. The fabrication process and cell conditions were the same as those for the IFDTN LC. Note that the LCs that were used did not have a chiral dopant different from conventional TN or ITN.

III. THEORETICAL MODEL

We numerically investigated the effects of anchoring strength on the director profile in ITN cells in which the LCs had no dopant. For simplicity, we assumed that the director orientations varied only along the z -axis, perpendicular to the substrates, and were constant in the x - y plane. The director profile was obtained by minimizing the Frank-Oseen free energy per unit area,

$$F_{\text{total}} = \frac{1}{2} \int_0^d [K_1 (\nabla \cdot \vec{n})^2 + K_2 (\vec{n} \cdot \nabla \times \vec{n})^2 + K_3 (\vec{n} \times \nabla \times \vec{n})^2 - \epsilon_0 \Delta \epsilon (\vec{E} \cdot \vec{n})^2] dz + F_s(z=0) + F_s(z=d), \quad (1)$$

where K_1 , K_2 , and K_3 are the splay, twist, and bend elastic constants, respectively, $\Delta \epsilon$ is the dielectric anisotropy, \vec{n} is the nematic director, \vec{E} is the applied electric field, ϵ_0 is the permittivity of free space, and d is the cell gap. The surface free energy density, F_s , for the director with alignment layer polar angle θ and azimuthal angle φ and an easy axis defined by a polar angle θ_0 and an azimuthal angle φ_0 is represented by the generalized Rapini-Popular equation²

$$F_s = \frac{1}{2} W_\theta \sin^2(\theta - \theta_0) + \frac{1}{2} W_\varphi \cos^2(\theta - \theta_0) \sin^2(\varphi - \varphi_0), \quad (2)$$

where W_θ and W_φ are the strengths of the polar and azimuthal anchoring energies, respectively. The relaxation method was employed to calculate the stable director orientations under the application of an electric field.¹⁷ The updated equations for the director field $\vec{n} = (\sin \theta \cos \varphi, \sin \theta \sin \varphi, \cos \theta)$ are

$$\theta^{\tau+1} = \theta^\tau - \alpha \left(\frac{\delta f}{\delta \theta} \right)^\tau \quad \varphi^{\tau+1} = \varphi^\tau - \beta \left(\frac{\delta f}{\delta \varphi} \right)^\tau, \quad (3)$$

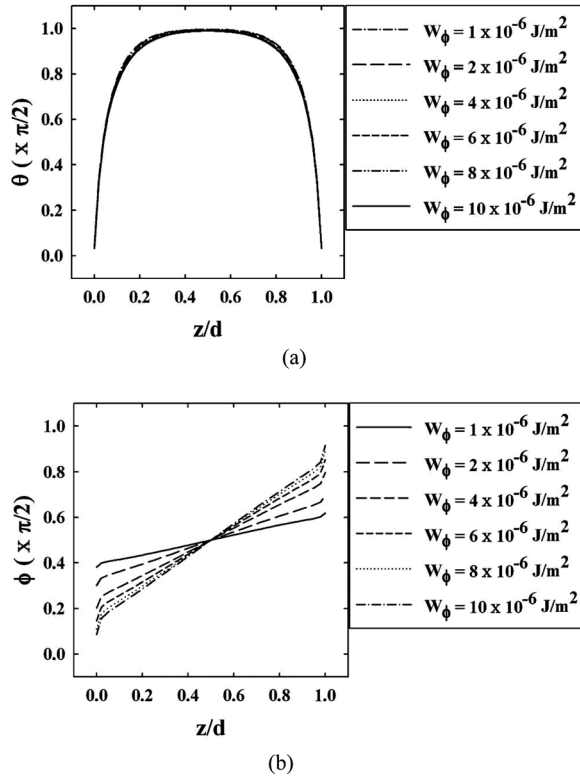


FIG. 3. Numerical calculations of the (a) polar angle and (b) azimuthal angle according to various azimuthal anchoring energies.

where f was the free energy density of the bulk region, α and β are the relaxation constants, and τ is the iteration index. Director orientations of the substrates were obtained according to the torque balance equations

$$\left(\frac{\partial f}{\partial(d\theta/dz)}\right)_{z=0,d} = p \left(\frac{\partial F_s}{\partial\theta}\right)_{z=0,d} \quad (4)$$

$$\left(\frac{\partial f}{\partial(d\phi/dz)}\right)_{z=0,d} = p \left(\frac{\partial F_s}{\partial\phi}\right)_{z=0,d},$$

where p is $+1$ at $z=0$ and is -1 at $z=d$.

Figure 3 shows the numerical calculation results for different azimuthal anchoring energies when 10 V was applied. The respective polar and azimuthal angles for easy axis were 3° and 0° for the bottom substrate and 3° and 90° for the top substrate, and the polar anchoring energy was assumed to be $W_\theta = 1 \times 10^{-3} \text{ J/m}^2$. The material parameters of the LCs used in this calculation are summarized in Table I. As shown

TABLE I. The material parameters of the LCs used in numerical calculation.

Parameters		Value
Elastic constants (pN)	K_1	16.7
	K_2	8.4
	K_3	18.1
Relative dielectric constants	$\epsilon_{ }$	3.62
	ϵ_{\perp}	7.7
Refractive indices (at 500 nm)	n_e	1.5586
	n_o	1.4756

in Fig. 3(a), the change in the polar angle with an increasing azimuthal anchoring energy was negligible. The profile of the azimuthal angle, however, changed significantly with changes in W_ϕ [Fig. 3(b)]. In the case of a relatively low azimuthal anchoring energy, $W_\phi = 1 \times 10^{-6} \text{ J/m}^2$, the LC molecules on both substrates rotated to minimize the elastic deformation, thereby producing a nontwisted, uniform alignment for the entire sample. With an increase in the azimuthal anchoring energy, rotation of the LC molecules on the substrates was prohibited due to the high anchoring force at the surface; therefore, the LC molecules are twisted. From these results, we determined that an alignment layer with a high azimuthal anchoring energy was a prerequisite for achieving an IFDTN structure. However, it has been reported that the azimuthal anchoring energy of a rubbed alignment layer is decreased 10^5 -fold with an increase in the pretilt angle from 2.8° to 88.4° .¹⁸ More recently, Kim *et al.* reported on the screening effect of surface anchoring energy by stacking a vertical alignment layer onto a planar alignment layer,¹⁵ suggesting that control and enhancement of the azimuthal anchoring energy may be achieved by adjusting the thickness of the vertical alignment layer on the planar alignment layer.

IV. RESULTS AND DISCUSSION

Figure 4 shows the azimuthal anchoring energies and textures of the samples with regard to the thickness of the

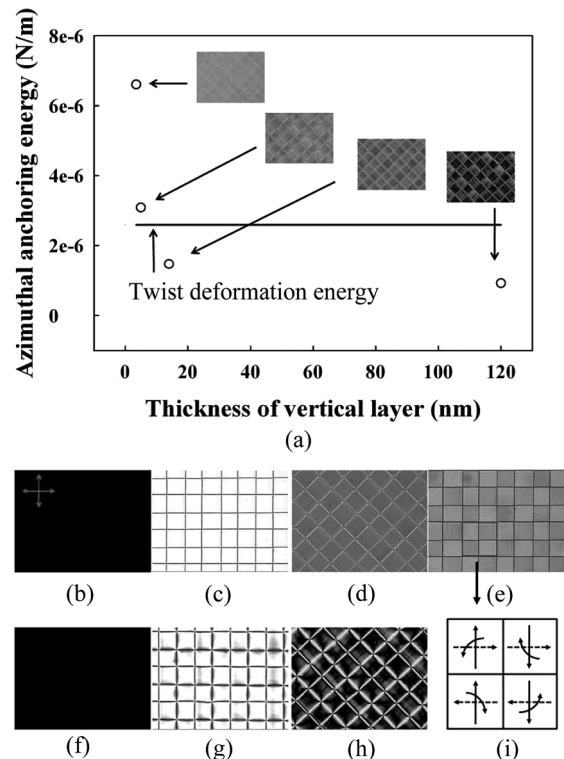


FIG. 4. (a) Measured azimuthal anchoring energies and textures of the samples under a polarizing microscope according to the thickness of the vertical alignment layer on the planar alignment layer, Textures of (b), (c), (d), (e) IFDTN samples with various stacked layers, (f), (g), (h) IFD samples with a single layer, and (i) the twisting direction of the IFDTN sample.

vertical alignment layer on the planar alignment layer, as determined using polarizing microscopy. The thickness can be controlled by the concentration of the vertical alignment material; by increasing the concentration of the vertical alignment layer, the azimuthal anchoring energy decreases. This results from the increasing thickness of the vertical alignment layer, which blocks the effect of the planar alignment layer. The textures were observed by rotating the sample by 45° with respect to the crossed polarizers at an applied voltage of 10V. The sample with a 5 wt % of vertical alignment material had an anchoring energy of 6.6×10^{-6} J/m² and displayed a uniform texture in each pixel. With an increase in the concentration of the vertical alignment layer however, the alignment of the LCs in each pixel became nonuniform as a possible result of a weakness in the azimuthal anchoring energy. The azimuthal anchoring energy of the pure vertical alignment layer was approximately 3.98×10^{-7} J/m², 17 times smaller than that of the stacked alignment layer with 5 wt % of vertical alignment material. The solid line in Fig. 4 indicates the twist elastic energy of the LCs, calculated using

$$F_{Twist} = K_2 \frac{\pi^2}{8d} = 2.59 \times 10^{-6} \text{ J/m}^2, \quad (5)$$

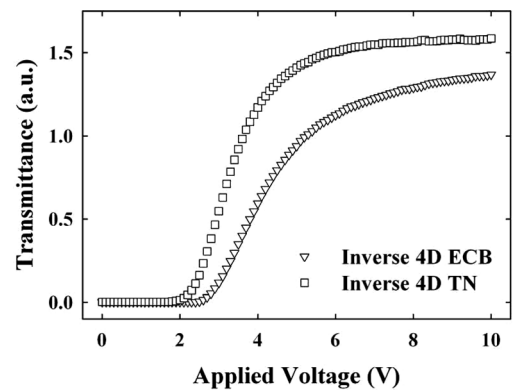
if it is simply assumed that the LCs are uniformly twisted in the sample without any other deformation. If the azimuthal anchoring energy is less than F_{twists} , then the LC molecules at the surface must rotate from the rubbing direction because it has to pay more energy to maintain the alignment. We believe that an anchoring energy greater than F_{twist} is required in IFDTN.

In order to obtain additional evidence of LC alignment, we observed the microscopic textures of the samples in each of the two extreme cases, as shown in Fig. 4. One sample was prepared by stacking a 5 wt % vertical alignment material onto the planar alignment layer [sample I]. The second sample was prepared with a pure vertical alignment material [sample II]. Both samples demonstrated a good dark state without the use of an external voltage due to the vertical alignment of the LCs, as shown in Figs. 4(b) and 4(f). When we applied 10 V, the LCs tilted, and both samples showed white states. Figures 4(c) and 4(g) show the respective textures of Samples I and II when the rubbing directions on the top and bottom substrates coincided with the crossed polarizers. The texture of sample I shows a very uniform alignment with sharp boundaries [Fig. 4(c)]. However, sample II shows a nonuniform alignment in each sub-pixel. Additionally, the boundaries in this sample are not well defined, which indicates the distribution of the LC alignment at the boundaries [Fig. 4(g)]. When we rotated the samples 45° , sample I showed very uniform textures in each sub-pixel and sharp boundaries, the same as in Fig. 4(c); the light intensity also decreased [Fig. 4(d)]. From the simulation and anchoring energy measurements, the LCs were known to be uniformly twisted in sample I, with an azimuthal anchoring energy of 6.6×10^{-6} J/m². The sharp boundaries indicated the different twisting senses.¹² Using a quarter-wave plate, we were able to observe different colors depending on the

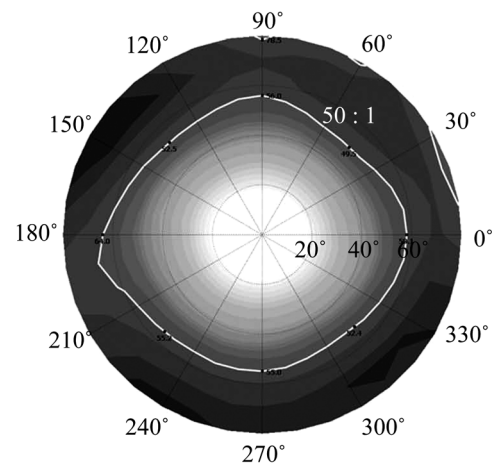
twisting senses, as shown in Fig. 4(e), where we presented a schematic diagram of the twisting directions in each sub-pixel in Fig. 4(i).

In contrast, sample II showed very complicated alignment textures when it was rotated by 45° [Fig. 4(h)]. The azimuthal anchoring energy of the pure vertical alignment layer was low, approximately 3.98×10^{-7} J/m², which is as low as to produce a nontwisted alignment, as shown in Fig. 4(a). Since each pixel had a different rubbing direction on the top and bottom substrates, the alignment was able to be deformed at the boundaries in order to minimize elastic deformation, which thereby propagates into the sub-pixel. Therefore, very complicated textures were obtained in each sub-pixel. From these results, we concluded that the sample with stacked alignment layers and the proper concentration of the vertical alignment material resulted in the formation of an IFDTN structure.

Figure 5 shows the electro-optical properties of the fabricated samples. The IFDTN with the stacked alignment layers shows an approximately 15% higher transmittance than that of the sample with vertical alignment layers only, as shown in Fig. 5(a). This is due to the well defined boundaries and uniformity of the LC alignment. In the conventional VA mode, a slow rising time is a



(a)



(b)

FIG. 5. (a) Measured voltage-transmittances and (b) viewing angle characteristics of the IFDTN sample. The white line inside the figure indicates a 50:1 contrast ratio.

major concern for TV applications; the tilting direction of the LC molecules is not clearly defined due to the very weak azimuthal anchoring energy with an applied electric field. In our proposed IFDTN mode, however, since the azimuthal anchoring strength was greater than that of the conventional VA mode, a faster rising time of 13.2 msec at a driving voltage of 6 V was observed. The viewing angle characteristics are presented in Fig. 5(b). The measurements were performed with commercial equipment (EZ-contrast, Eldim). In order to reduce the off-axis light leakage at 0 V, a bi-axial compensation film was attached during the measurements. The white line in Fig. 5(b) indicates a 50:1 contrast ratio. It is evident that wide and symmetric viewing characteristics were achieved in the proposed IFDTN sample.

V. CONCLUSIONS

We fabricated the first IFDTN LCD through the enhancement of the azimuthal anchoring energy of the alignment layer by stacking a vertical alignment layer onto a homogeneous alignment layer. The anchoring energy of the stacked alignment layers increased by approximately 17-fold compared to that of the vertical alignment material alone. Due to the enhanced azimuthal anchoring energy, we were able to achieve a four-domain twisted nematic LC structure without dopant through the application of an external voltage. The fabricated IFDTN LCD shows wide and symmetric viewing characteristics which are appropriate for large LCDs. We have determined that the simplest way to fabricate an IFDTN is by using a photo-alignment technique, as mentioned introduction section, and is dependent on the

development of the proper vertical alignment materials with high azimuthal anchoring energies.

ACKNOWLEDGMENT

This work was supported by Samsung Electronics Co. Ltd.

- ¹M. Schadt and W. Helfrich, *Appl. Phys. Lett.* **18**, 127 (1971).
- ²J. S. Patel and G. B. Cohen, *Appl. Phys. Lett.* **68**, 25 (1996).
- ³M. Oh-e and K. Kondo, *Appl. Phys. Lett.* **67**, 3895 (1995).
- ⁴S. H. Lee, S. L. Lee, and H. Y. Kim, *Appl. Phys. Lett.* **73**, 2881 (1998).
- ⁵A. Takeda, S. Kataoka, T. Sasaki, H. Chida, H. Tsuda, K. Ohmuro, T. Sasabayashi, Y. Koike, and K. Okamoto, SID'98 Tech. Dig. **29**, 1077 (1998).
- ⁶K. Sueoka, H. Nakamura, and Y. Taira, SID'97 Tech. Dig. **28**, 203 (1997).
- ⁷J. Chen, P. J. Bos, D. R. Bryant, D. L. Johnson, S. H. Jamal, and J. R. Kelly, *Appl. Phys. Lett.* **67**, 1990 (1995).
- ⁸M. J. Escuti, C. S. Bowley, G. P. Crawford, S. Zumer, *Appl. Phys. Lett.* **75**, 3264 (1999).
- ⁹M. Schadt, K. Schmitt, V. Kozinkov, and V. Chigrinov, *Jpn. J. Appl. Phys.* **31**, 2155 (1992).
- ¹⁰M. Schadt, H. Seiberle, and A. Schuster, *Nature* **381**, 212 (1996).
- ¹¹H. Seiberle and M. Schadt, SID'97 Tech. Dig. **28**, 397 (1997).
- ¹²J. Chen, P. J. Bos, D. L. Johnson, D. R. Bryant, J. Li, S. H. Jamal, and J. R. Kelly, *J. Appl. Phys.* **80**, 1985 (1996).
- ¹³K. Miyachi, K. Kobayashi, Y. Yamada, and S. Mizushima, SID'10 Tech. Dig. **41**, 579 (2010).
- ¹⁴S. Varghese, G. P. Crawford, C. W. M. Bastiaansen, D. K. G. de Boer, and D. J. Broer, *Appl. Phys. Lett.* **86**, 181914 (2005).
- ¹⁵M. S. Nam, J. W. Wu, Y. J. Choi, K. H. Yoon, J. H. Jung, J. Y. Kim, K. J. Kim, J. H. Kim, and S. B. Kwon, SID'97 Tech. Dig. **28**, 933 (1997).
- ¹⁶Y. J. Lee, J. S. Gwag, Y. K. Kim, S. I. Jo, S. G. Kang, Y. R. Park, and J. H. Kim, *Appl. Phys. Lett.* **94**, 041113 (2009).
- ¹⁷H. Mori, E. C. Gartland, Jr. J. R. Kelly, and P. J. Bos, *Jpn. J. Appl. Phys.* **38**, 135 (1999).
- ¹⁸H. Mada, and S. Saito, *Jpn. J. Appl. Phys.* **38**, 1118 (1999).